



ELSEVIER

Microbeam AMS: prospects of new geological applications

S.H. Sie^{*}, T.R. Niklaus, G.F. Suter

Heavy Ion Analytical Facility, CSIRO Exploration and Mining, P.O. Box 136, North Ryde, NSW 2113, Australia

Abstract

AMS applications in geology have hitherto concentrated on the use of cosmogenic isotopes and rare in-situ produced isotopes for geomorphological and geophysical studies. Special features of AMS lend themselves to more general applications to other isotopes and geochronological systems. In-situ measurements in geochronology carried out with ion-microprobes are restricted by isobaric and molecular mass interferences to special systems where the problem is minimal. AMS can be used to alleviate this mass interference problem, and opens up the prospect of a less restrictive in-situ microanalysis for geochronology. At CSIRO, a microbeam AMS system designed to achieve this capability is under construction. With this system, several interesting applications such as the Re–Os system became accessible more conveniently. The U–Pb system becomes accessible for hydrous minerals, and Rb–Sr systems for Rb-rich samples. In addition, microbeam AMS allows determination of trace elements at lower levels than those accessible with the proton microprobe. This paper discusses these prospects and describes the AUSTRALIS system (AMS for Ultra Sensitive TRAce eLement and Isotopic Studies) being developed at CSIRO.

1. Introduction

Since its inception, geological applications of accelerator mass spectrometry (AMS) have been predominantly concentrated in the exploitation of cosmogenic isotopes in geophysical and geomorphological problems. The key advantages of AMS, namely the ultra sensitivity (as low as 10^{-15} in isotopic abundance) and the minute sample (as low as 200 μg) requirement, opened up new windows of opportunity. Ice cores can be analyzed with higher time resolution providing an unprecedented detailed record of past climatic changes. Atmospheric and oceanic circulation can be studied with greater spatial resolution which will enable improvements in climate prediction capability. In-situ produced nuclides can be used to measure exposure ages and erosion rates [1].

Applications in geology proper however are not as well developed but are growing steadily. AMS potential in geochemistry as a trace analyzer for precious metals such as the platinum group elements (PGE), Au and Ag [2–5], with sensitivity at or better than crustal abundances, and in isotope geology [6–8] for isotope ratios measurements at the percentile precision level, have been demonstrated using the “bulk” or “milliprobe” approach. The potential

of a more generalized application using other radiogenic or stable isotopes has long been recognized through the kinship of AMS with the older technique of SIMS (secondary ion mass spectrometry).

SIMS has developed into an established tool in some specific areas of geochronology and trace element studies [9] through the inherent high efficiency of mass spectrometry versus radiation based spectroscopy, but particularly because of the development of the ion microprobe. In-situ microbeam techniques obviate laborious mineral and chemical separation in analysis of complex assemblages of microscopic monomineralic constituents typical of geological samples, and enable analysis of micro-samples (e.g. inclusions) and micro-features such as zoning in minerals. Severe molecular and isobaric interferences arising from the complex matrix have prevented the general application of the ion microprobe in geochronology, except for special cases such as the U/Pb system where there is no parent–daughter interference and when molecular interference is minimized in anhydrous matrices such as zircons. The energy filtering method [10] has been successfully used to reduce molecular ions by exploiting their narrower kinetic energy distribution compared to that of the atomic ions. By setting an electrostatic analyser to pass the higher energy “tails” of the atomic ions, molecular ion suppression is achieved but at the expense of lower efficiency. The other approach focuses on the development of an ever higher mass resolution spectrometer [11,12] through higher order beam optics design in order to minimize aberration effects

^{*} Corresponding author. E-mail s.sie@dem.csiro.au; tel. +61 2 887 8648; fax +61 2 887 8921.

[13,14]. The mass resolution of ~ 27000 attainable in such a spectrometer [14] will resolve hydride interference in the mass region 200, but isobaric interference problems are still not resolvable.

Molecular interference is eliminated by AMS, and the same process can be used to resolve isobaric interference by selecting appropriate molecular ions for injection. The use of negative ions also offers a number of discrete advantages in selected cases.

As a "bulk" analyzer, AMS is not viable in terms of precision and unit cost of analysis against thermal ionisation mass spectrometry (TIMS) in isotope geology, and against ICP-MS (inductively coupled plasma source mass spectrometry) as a trace analyzer, except in cases involving sub-ppb sensitivity. The advantages of AMS must be delivered in a spatially resolved approach, thereby improving on the advantages offered by the ion microprobe. This provides the impetus for the development of AUSTRALIS (AMS for Ultra Sensitive TRAce eLement and Isotopic Studies), a microbeam-AMS suitable for in-situ microanalysis of ultra traces and of isotopic data in geological samples, at the HIAF laboratory at North Ryde, Sydney [15,16]. The laboratory, based on a 3 MV Tandem accelerator, is dedicated to applications of ion beam techniques in minerals research [17–19]. This paper presents an overview of general considerations of a microbeam AMS system, and of the prospects of its new applications in geology, with emphasis on mineral exploration research.

2. Microbeam AMS constraints

It is instructive to use ^{14}C as a starting point to identify the boundaries of the applicability of a microbeam AMS system from the method and instrumental viewpoints. In a typical Tandem based AMS operating at 2 MV, modern samples containing ^{14}C at $\sim 10^{-12}$ concentration yield ~ 2 counts per second of $^{14}\text{C}^{3+}$ per μA of injected C^- beam. To obtain a 1% statistical precision a minimum of 10^4 counts is needed. The minimum amount of carbon required depends on the ionisation efficiency which for graphite could be as high as 8%, translating to $\sim 10^{-6}$ mol of carbon with a volume of $\sim 5 \times 10^6 \mu\text{m}^3$. This relationship can be generalized to indicate the minimum required mass or volume of the matrix for achieving a given statistical precision for the detection of an isotope occurring at a given concentration. Fig. 1 shows this as the anchor point that defines the iso-concentration line corresponding to 10^{-12} concentration. A family of lines can be generated easily for other concentrations. The volume is relevant from the microbeam analysis consideration. It is not advisable that the depth of the sputtered well should be greater than the lateral dimensions, and thus the cube root of the volume represents the smaller lateral dimension of the beam. Using this assumption, and arbitrarily defining a microbeam as that with less than $100 \mu\text{m}$ lateral dimen-

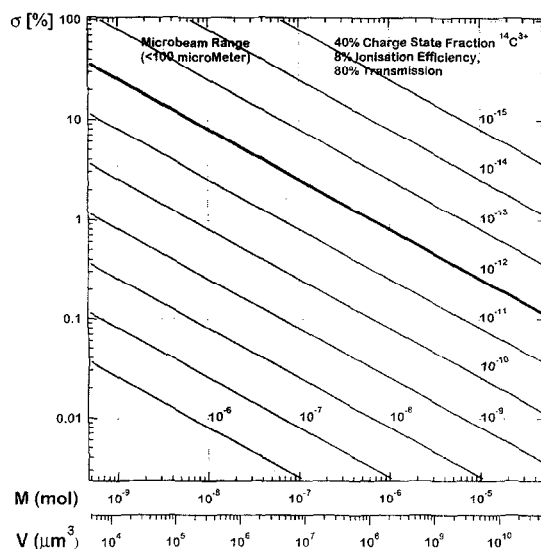


Fig. 1. Diagram showing the relationship between the required statistical precision and the minimum amount of sample material required, for various given concentrations of the isotope to be measured and an 8% ionisation efficiency for detection of ^{14}C from pure modern carbon ($\sim 10^{-12}$ concentration) in 2 MV Tandem AMS systems. The material axis can be expressed also as volume of the material. The regime of microbeam measurements, defined as that carried out with a beam having diameter $< 100 \mu\text{m}$, can be defined assuming an aspect ratio of depth vs. diameter of < 1 . A similar diagram can be generated for an isotope in any given matrix when the ionization efficiency is known.

sion, an upper boundary in volume or mass can be defined. The precision required defines the upper boundary on the ordinate, and the two boundaries together with the concentration requirement define the regime of possibility of microbeam measurements.

The second consideration relates to the feasibility from the data collection time viewpoint. Fig. 2 shows the time vs. primary ion beam intensity, assuming that the ionisation yield is known, for a series of required statistical precision values for detecting an isotope occurring at 10^{-12} concentration. If we assume an ionisation yield of 10% for $^{12}\text{C}^-$ from graphite [20], the primary beam intensity is thus ~ 10 times the intensity of the total negative current from the graphite matrix.

The third consideration defines the attainable primary beam intensity for a given beam diameter. In the absence of known measured emittance of the primary beam, we can use empirical beam density values. In a HICONEX source, as much as $100 \mu\text{A}$ Cs^+ beam can be focused to ~ 0.3 mm, corresponding to $\sim 140 \text{ mA}/\text{cm}^2$ beam density. In this source, we can safely assume that the focus is highly aberrated, and thus the beam density represents the lower limit. Neglecting effects of lens aberrations, the beam density is a constant. Towards the lower values of beam

diameter, the beam density can drop due to aberration effects, or improve because of the better beam phase space distribution for paraxial rays. But for the purpose of the present consideration the relationship applies to better than a factor of 2 or 3.

The two graphs and beam density consideration enable us to draw some conclusions. With a 1 μA primary beam, the beam diameter is at least 30 μm , and the total secondary ion beam intensity is 0.1 μA . A 1% precision measurement requires $\sim 5 \times 10^4$ s for each isotope with a 10^{-12} concentration. If the practical measuring time is set at 60 s, the sensitivity drops to 10^{-9} , in which case Fig. 1 would indicate that the material available is not the limiting factor. For a sensitivity of 10^{-10} , a minimum measuring time of 600 s is needed, and the amount of material required is such that the “cylinder” has a length bigger than the beam diameter, which is not desirable. A wider beam would be recommended, or the beam should be scanned over a larger area.

Figs. 1 and 2 represent the best condition, unlikely for typical geological samples. The figures would vary with the matrix and elements of interest, and with ionization efficiencies, shifting by a few orders of magnitude towards the less sensitive direction, but the procedure of assessment of sensitivity would be similar. In view of this, microbeam AMS applicability for 0.1% precision isotopic ratio measurements would be confined to, at best, isotopes occurring at $\sim 10^{-9}$ concentration. For trace element

measurements, the statistical precision is considerably more relaxed, and thus at say 10% precision concentrations at 10^{-13} can be attained with a microbeam under favourable conditions. These are to be compared with the current state-of-the-art of ion microprobe measurements where with a 20–30 μm primary beam, isotopic ratios with precision in the % regime (e.g., Pb isotopes) can be measured at Pb concentration ≥ 20 ppm [11,12].

Similar considerations in SIMS have been presented previously, mainly in terms of the ultimate detection limit for trace analysis, and depth profile resolution for a given beam spot size [21–23]. Isotopic analysis for geochronological applications in AMS as discussed above poses more stringent limits on the feasibility of microbeam measurements.

3. Instrumental constraints

3.1. Ion source energy stability

The statistical precision represents the upper limit of reproducibility and accuracy of the results. Fractionation effects can be induced by instabilities of the ion source, beam transport and the accelerator itself. The secondary ions kinetic energy distribution becomes a very important factor when reproducibility in the 0.1% regime is required. The effect has been demonstrated in ion microprobe measurements where, for example, for a 50 eV change in energy, the isotope ratio can change by a factor of 5 reflecting the change in the molecular fraction of the mass of the ions measured [10]. For an extraction energy of ~ 10 keV this corresponds to 0.5% energy difference. In macrobeam AMS it would be difficult to obtain a high energy resolution for a given mass, as reflected in the width of the “flat-top” transmission, of greater than say 600. For a typical double focusing magnet with radius $R = 30$ cm this would require a beam width of 1 mm at the image and object. The object in turn is the image of the source, and assuming that the source is more likely than not magnified by the extraction lens system in order to reduce its emittance to match the acceptance of the magnet, the object size must be less than 1 mm. If the magnet is operated at higher resolution by closing down the object slits, there will be an uncertainty in energy compounded by the loss of transmission efficiency.

Better control of the energy distribution can be achieved with the insertion of an electrostatic analyser prior to the magnetic analysis. A 45° bend spherical electrostatic analyser operating in the double focusing mode has a dispersion of $2R$. If operated at unity magnification, with object and image distance of $(\sqrt{2} + 1)R$, a 30 cm radius electrostatic analyzer (ESA) can achieve an energy resolution of 600 with 1 mm slits.

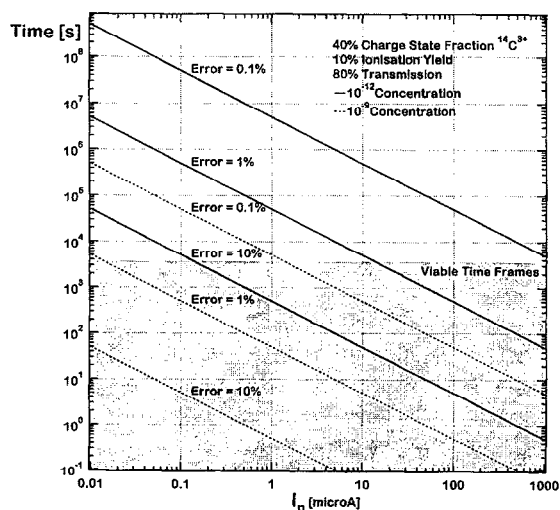


Fig. 2. Diagram showing the relationship between the primary beam intensity and the required measurement time, for various required statistical precisions (“error”) for a given concentration of 10^{-12} (solid lines), based on 10% ionisation yield. The shaded area defines the viable measurement times, shown here arbitrarily as < 1 h. Similar curves for other concentrations, e.g. for 10^{-9} (dashed lines), and ionisation efficiencies can be generated from the solid curves.

3.2. Accelerator stability

At the high energy end, the requirement for analysis of heavy elements up to the actinides governs the size of the magnet. To analyze charge 5^+ of mass 240 at accelerating voltage of 2.5 MV a magnet of beam product (mE/q^2) of 144 MeV amu is required. The radius is determined by the required magnet gap given the maximum field that can be achieved. The gap size in turn must be matched with the divergence of the beam out of the accelerator. For ~ 3 cm gap, this beam product can be achieved with a 1.3 m radius magnet. When used in the double focusing, unity magnification mode, the dispersion length of this magnet would be $2R = 2600$ mm. Thus with an object slits setting of 1 mm, the mass resolution is 2600. The equivalent energy stability for a given mass setting is thus $1/2600 = 3.8 \times 10^{-4}$. In principle, Tandetrans are capable of 10^{-4} terminal voltage stability, corresponding to 250 V ripple at 2.5 MV terminal voltage. But, in practice, with only a GVM (generating voltmeter) stabilisation, the difficulty in obtaining a stable reference voltage results in instability at least twice that, which is comparable to that required for maximum energy resolution of the magnet. However slow drifts of the terminal voltages can exceed this value, and thus for high precision measurements either a multi-Faraday cup, a position sensitive Faraday cup [24] and/or a fast isotope sequencing method is required. A multi-Faraday cup system requires a broad range magnet, but for suppression of background from other molecular fragments, it must be preceded by an electrostatic analyser. A position sensitive Faraday cup is useful if a major isotope is available for the particular measurement.

Fast sequencing is the more universal method, and can be implemented by modulating the orbit of the different isotopes by transverse displacement in the orbit plane, using pairs of electrostatic deflectors with low energy storage at the entrance and at the exit end of the magnet. This method was developed originally as an energy modulator by Amsel et al. [25].

3.3. Microbeam production

Production of microbeams is aimed at the best resolution at the best intensity, within the limits imposed by the source brightness and stability, by controlling aberrations in the probe forming system. While parasitic aberration can be minimized by setting high tolerances in the lens construction, spherical aberration control can be limited by other than beam optical considerations, e.g. space restrictions. Surface ionisation sources, which are the most common type used for Cs beam production, tend to have poor brightness compared to field emission sources. The space charge effect would ultimately limit the beam density that can be achieved in a microbeam.

For low energy beams, electrostatic cylindrically symmetric lenses are preferred because of their simple optical

properties and construction. Practical limits are set by the vacuum breakdown potential and as a rule gradients less than 30 kV/cm should be observed. At moderate spatial resolutions ($> 1 \mu\text{m}$) spherical aberration is more important than chromatic aberration.

The available working distance defines the focal length of the microbeam lens. For a highly demagnified image, the image distance approaches the focal length f . For cylindrical lenses, with bore b greater than the sum of the length d and the gap a [26]:

$$f = b^2 / (d + a) \sim b.$$

The lens bore should therefore be just smaller but comparable to the working distance, and to minimize spherical aberration effects the working distance should be as low as possible. The bore can be further constrained by the need to accommodate the secondary ion extraction lens. The effect of spherical aberration is best estimated using ray tracing techniques. In an accompanying paper [27], ray tracing using the program SIMION [28] presents the results for a microbeam lens system corresponding to a working distance of ~ 40 mm and a microbeam lens with 25 mm bore. The ray trace shows that the image becomes highly aberrated for object size > 1.0 mm diameter. For an object size of < 0.5 mm diameter the image size is $\sim 20 \mu\text{m}$, increasing to $\sim 300 \mu\text{m}$ for a 1 mm diameter object. For surface ionizers, a beam density of $\sim 2 \text{ mA/cm}^2$ can be obtained [29]. The maximum intensity at 20 μm resolution that can be achieved with the system shown in Ref. [27] is thus $\sim 4 \mu\text{A}$, assuming all rays are focused as shown, corresponding to 1270 mA/cm^2 . In practice, a slightly worse performance would be obtained due to other effects, e.g. poor surface texture of the ionizer which will increase beam divergence. This can be inferred by comparing the beam density to the $\sim 140 \text{ mA/cm}^2$ obtained in a typical HICONEX source. It is therefore reasonable to assume that a 1 μA beam intensity can be achieved at 30 μm resolution.

4. The instrument

The design of AUSTRALIS is governed by the anticipated applications, and the constraints discussed previously. From our previous experience in designing a proton microprobe for geological applications [18], a working beam resolution of $\sim 10\text{--}30 \mu\text{m}$ was arrived at by balancing the typical depth of analysis, and the need to obtain sufficient beam intensity for practical measurement time (less than ~ 15 min per spot analysis). With this spatial resolution we can analyze most geological samples with parts-per-million sensitivity for trace element detection. AMS analyzes the surface region and hence the effective depth of analysis argument does not apply, and the beam resolution limits are determined more by the availability of

Table 1
Design specifications of "AUSTRALIS"

Mass analysed Cs microbeam
Spatial resolution $< 30 \mu\text{m}$; ultimately $< 1 \mu\text{m}$
Cs beam intensity $> 1 \mu\text{A}$ at $30 \mu\text{m}$; 10nA at $1 \mu\text{m}$
Sample viewing with $> \times 100$ magnification; $1 \mu\text{m}$ pixel
Low aberration low energy beam transport
Spherical electrostatic analyzer (45°) $E/\Delta E > 600$ and magnetic analysis $M/\Delta M > 600$ at low energy side
High energy analyzing magnet: beam product ≥ 140 , $M/\Delta M > 1500$
Spherical electrostatic analyzer at high energy side

material and the beam intensity. Ultimately, the feasibility is determined by the precision required.

A practical feature which becomes important especially when minute samples are analysed, e.g. inclusions, is the ability to position the beam on the sample accurately. This can be achieved using a computer controlled microstage

for the target mounting, and a facility to view the samples at high magnification ($> \times 150$). The same viewing system can be used to ensure that the sample is always positioned at the same distance from the extraction optics to guarantee reproducibility. Further practical considerations include target position stability at much lower dimension than the beam resolution, and a facility to insert and remove targets through a vacuum lock.

A mass analysed Cs beam is desirable to minimize contamination of the sample, especially when alkali elements are to be analyzed. Other considerations to improve precision of the measurements include a low aberration beam transport system for the injector in order to achieve the best mass and energy resolution. The main specifications of the AUSTRALIS system are summarized in Table 1.

A preview of the implementation of the specifications has been presented previously [15]. Fig. 3 shows a diagram of the actual ion source and injector system. In the first

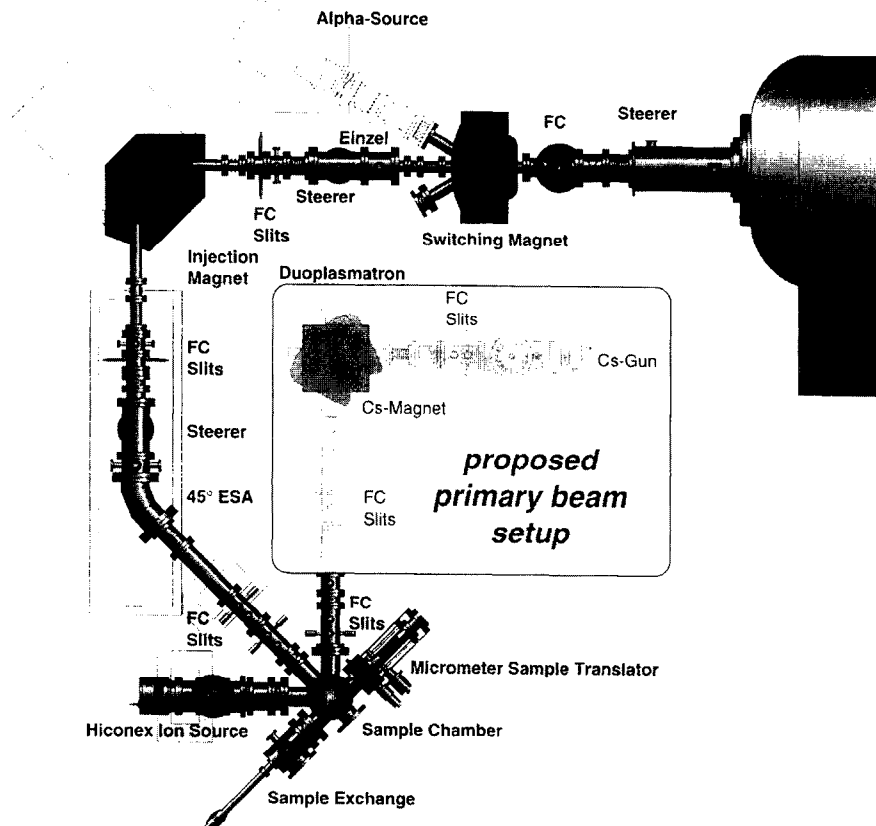


Fig. 3. Plan view of the AUSTRALIS injector system. The sample is mounted on a three axis microstage. The primary microbeam from the modified HICONEX source strikes the sample at 45° incident angle. The secondary ions extracted at normal angle are focused by einzel lenses and passes through a 45° spherical electrostatic analyser (ESA) and a 90° double focusing magnet for injection into the accelerator. A second, mass analyzed ion source will be added in the future.

stage, the microbeam source is developed from an existing HICONEX source. The mass analyzed Cs source will be added in the future. The system and the test results are described in greater detail elsewhere in these proceedings [27].

The microbeam strikes the sample mounted at the centre of the chamber on a three axis microstage, at 45° from the target normal. Following the technique used in ion-microprobes when a positive primary beam is used, an electron flood gun is mounted on the other 45° to compen-

sate for charge build-up on insulating targets (e.g. silicates). The secondary ions are extracted at normal angle, and focused by an immersion einzel lens followed by another lens at the first set of slits to form the object for a double focusing, 45° bend spherical ESA with a 30 cm mean radius and 3 cm gap set for unity magnification. A second set of slits follows the Faraday cup, designed to reduce beam halo. The ESA image is the object for a high resolution, double focusing 90° magnet corrected to the second order, with a 30 cm mean radius and 2.5 cm gap.

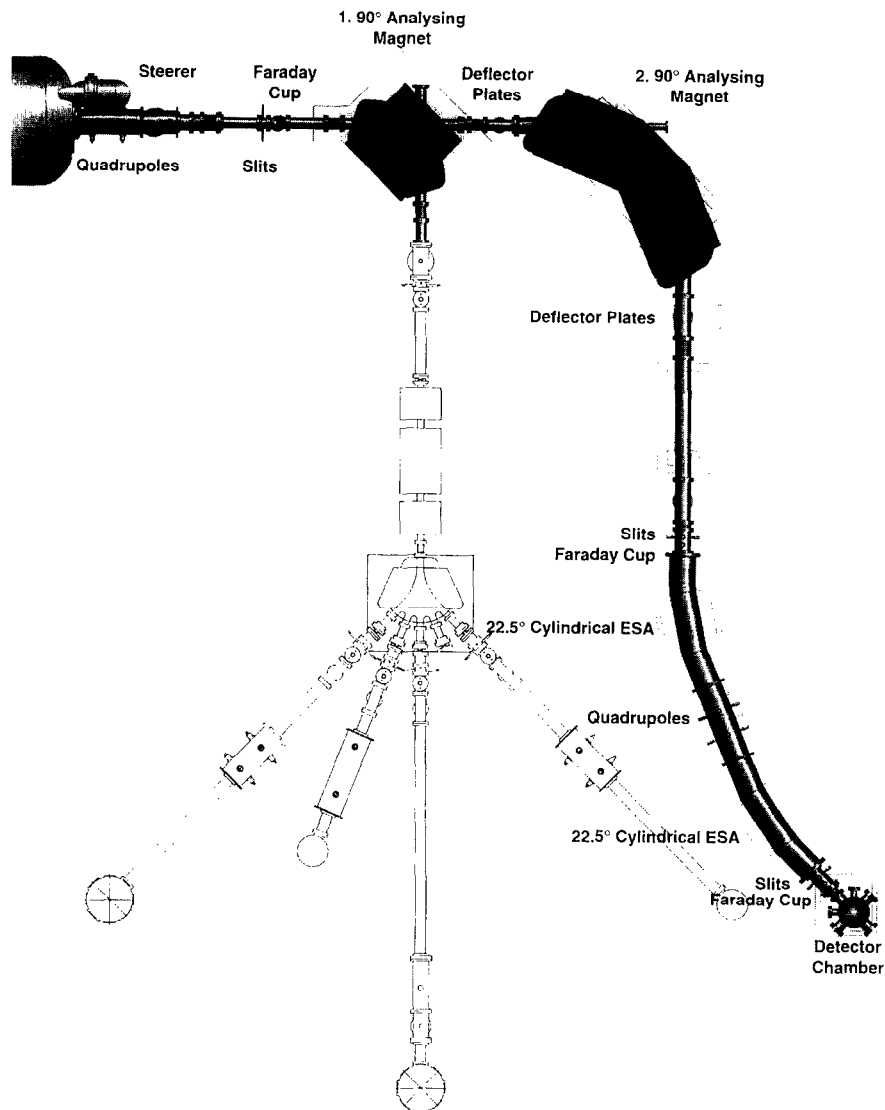


Fig. 4. Plan view of the high energy analysing system. The beam passes through a demagnetized magnet (1) into a 90° double focusing Danfysik magnet (2) with a beam product of 140 MeV amu . The beam is further transported through two 22.5° ESAs separated by an electrostatic quadrupole doublet and focused into the detector chamber. The electrostatic deflector plates at the entrance and exit ports of the magnet form the high energy bouncing system.

Since the secondary ions are produced by microbeams, the ESA and the magnet can be operated with narrow slit settings. At 1 mm slit setting an energy resolution of 600 and a mass resolution of 600 will be obtained with this injector system. The magnet beam box is insulated to permit the usual “bouncing” technique, namely modulation of the beam energy for different isotopes to maintain the same bending radius, by applying appropriate voltages to the box. The beam is further transported to the accelerator through the 0° port of a three way switching magnet, with two einzel lenses for control of the beam envelope and matching it to the acceptance of the accelerator. All beam transport elements are computer controlled facilitating optimisation of the settings for maximum transmission and resolution [27].

Fig. 4 shows a diagram of the high energy system. In the AUSTRALIS mode of operation, the beam by-passes the existing small analysing magnet, using its straight through port and enters a 90° double focusing magnet with 1.3 m radius. The magnet is located such that its object coincides with the object slits of the existing magnet. The new (Danfysik) magnet is corrected to the second order and its nominal maximum beam product (mE/q^2) is 140 MeV amu, but it can be operated up to 10% above specification, permitting analysis of mass 240, 5+ ions at ~2.5 MV terminal voltage or 4+ at ~2 MV. The 3 cm gap and 15 cm wide pole tips accommodate a 10 cm wide by 2.5 cm high stainless steel beam box, allowing at least ± 10 amu latitude in transmission at mass 240 and matching the vertical acceptance of the magnet to the emittance at the high energy. The magnet current is powered by a Danfysik model 858 current supply regulated to 1 ppm.

The fast isotope sequencing system consists of two sets of deflecting plates, 40 cm long with 4 cm gap, at the entrance and the exit ports of the magnet box. Different isotopes are deflected by different amounts transversely in the orbit plane by the entrance plates and returned to the main axis by the exit deflectors by applying common voltages to both sets, without altering the magnetic field setting. Preliminary tests with a proton beam (3–3.06 MeV) in the energy modulating mode indicate a flat transmission over the energy range of up to 1.2% from the mean value, corresponding to a similar range in mass difference when used as an isotope switcher. The test was carried out by first optimising the beam in the magnet Faraday cup with no deflecting voltage. A given voltage was applied to the plates until the beam current dropped to zero. The accelerator terminal voltage was then adjusted to restore the beam in the cup. With the slits set at ± 1 mm width there is no current registered at the slits. Fig. 5 shows a plot of the deflector voltage vs. the accelerator terminal voltage from the test, and the calculated values as a function of the effective mean distance of the plates from the field boundary.

A dynamic test with heavy isotopes at a fixed terminal voltage awaits the installation of a terminal pumping sys-

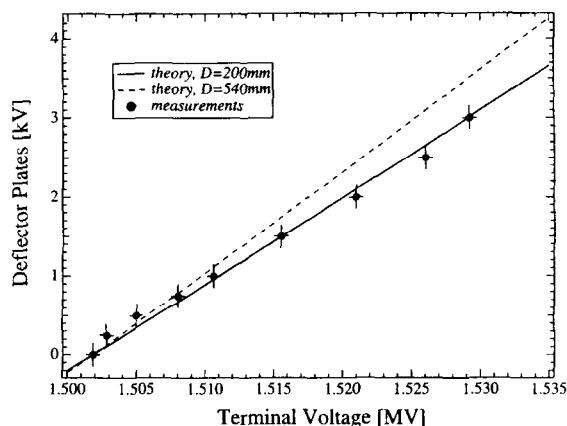


Fig. 5. The high energy bouncing system was tested using a proton beam between ~3 and 3.06 MeV. The plot shows the deflector plate voltage versus the proton beam energy represented by the terminal voltage, and the calculated values for various distances D representing the mean distance of the deflector plate to the magnetic field boundary.

tem, and the delivery of fast switching high voltage power supplies for the deflector. Switching rise time in the tens of microseconds and cycle times in the milliseconds are envisaged to minimize the effect of drifts in the system. The cycle time however may have to be extended for low yield counting. The precision obtainable will ultimately be limited by possible heterogeneity of the sample itself at the microscopic scale of the analyzed volume. Simultaneous injection of the isotopes, e.g. directly or using a recombinator injector system, may eliminate the uncertainties in sequential injection, but these techniques are not without problems, especially when the isotopes of interest are in the vicinity of major or even minor elements of the matrix.

Following the magnet the beam passes through two 3 m radius, spherical ESAs with 22.5° bend, separated by an electrostatic quadrupole doublet. Space limitations prevent the use of the ESA as double focusing devices, necessitating the quadrupole lens to focus the beam at the detector chamber at a reasonable distance. The quadrupole is set between the two ESAs to maintain the beam envelope below 25 mm, and to keep the maximum voltages of the ESA below 50 kV in order to minimize hazardous X-ray background. The quadrupole focuses the beam into either a Faraday cup or an ion detector, which can be a proportional counter. A time-of-flight system will be implemented by installing a start detector at the entrance to the first ESA.

5. Prospects of applications

5.1. Ultra-trace measurements

As a trace analyzer, AMS suffers the same problem as the ion microprobe and laser ablation ICP-MS methods, namely the need of standards for quantification because of

the uncertain matrix effects. The relative yield method [10,30] has greatly aided the problem of quantification. Despite this, there can still be unexpected effects such as the dependence of the relative yield on the crystallinity of the samples [31]. It is therefore imperative that new types of samples should be cross calibrated against another known quantitative techniques. Foremost among these is the proton microprobe, which can be used to analyze the same analytical spot non-destructively, with sensitivity in the ppm regime.

The advantage of microbeam AMS versus the ion microprobe lies in its higher sensitivity, arising from the intrinsically higher transmission and detection efficiency of AMS in not requiring a very high mass resolution, although some of this may be diminished by the charge exchange process in AMS. Against the laser ablation probe, microbeam AMS gains in overall efficiency and sensitivity. The ICP-MS end of a typical laser microprobe operates with a detection efficiency of 0.2% versus 3% in AMS [32] and for a beam resolution of $> 30 \mu\text{m}$ the minimum detection limit is ~ 0.5 ppm for a wide range of elements [33].

The sub-ppm sensitivity of AUSTRALIS will be applied to problems currently inaccessible by the proton microprobe. In most silicates, the PIXE detection limits for trace elements lighter than Fe are generally poor (> 100 ppm), because of the ubiquitous presence of Fe and the limitations imposed by the use of energy dispersive spectrometers (Si(Li) detectors) [18]. Many light elements are important geochemical markers, and in-situ detection of these at sub-ppm levels will become possible by AMS. Similarly, PIXE sensitivity for heavy elements is poor because of lower X-ray yield, low detection efficiency and overlapping peaks. AMS has been shown to have detection limits in the sub-ppb to ppb range for PGE and Au, and comparable sensitivity is expected for other elements. AUSTRALIS will facilitate measurements of PGE and rare-earth-elements (REE) fractionation patterns in petrogenetic studies, and the more practical applications of precious metal distribution in coexisting ore minerals for ore processing. Analysis of heavy minerals (e.g. tetrahedrite, monazite, zircon) will also benefit from the absence of background due to the high-Z matrix. The high sensitivity is crucial in analysis of mantle minerals (olivine, garnets, spinels, pyroxenes), which are generally depleted with the majority of trace elements occurring at the sub-ppm level. The ultra-sensitivity of AMS facilitates measurements of partition coefficients, e.g. between sulfides, silicates and carbonates, at much lower levels of trace elements which will improve our understanding of magma generation and subsequent evolution. Mantle metasomatism, alteration of rocks by melts or fluids, can be studied in better detail to understand the nature and origin of the metasomatising agent. Micro-AMS will facilitate studies of microscopic relics of primitive magma, trapped as inclusions in minerals, with greater sensitivity.

5.2. Isotopic measurements

In isotopic studies, micro-AMS will be constrained by the attainable precision as limited both by the abundance concentration of the isotopes of interest as well as the intensity of the microbeam. The common Pb and U/Pb applications require the order of 1% precision in the isotopic ratios measurements. Ion microprobe measurements are limited to anhydrous minerals to avoid the hydride ion interference on the ^{207}Pb isotope measurement. Micro-AMS eliminates this constraint, and at the level of precision required, the Pb isotopes data are likely to be obtained from minerals containing Pb as low as 1 ppm.

With the facility to suppress interfering ^{87}Rb by selecting negative Sr hydride ions, micro-AMS enables analysis of Sr isotopes in high Rb phases, such as micas. Even in carbonates, where the Rb interference is low, micro-AMS offers an advantage over the ion microprobe measurement by eliminating interference from Ca_2 and CaMgO molecules [34]. The expected variation in $^{87}\text{Sr}/^{86}\text{Sr}$ is reasonably large: from ~ 0.70 in chondrites to 0.714 in continental samples. A precision in the 0.3% regime will allow useful discrimination in some petrogenesis studies. The microbeam limits will restrict measurements to minerals with a Sr content of ≥ 10 ppm.

The $^{187}\text{Re}-^{187}\text{Os}$ system is potentially a powerful tracer for mantle differentiation processes as well as a sensitive geochronometer. From a ratio of ~ 1 , Re/Os is highly fractionated during magma generation, with Re partitioning mainly into the melt, resulting in its enrichment in the crust (Re/Os ~ 3000). The effect on the $^{187}\text{Os}/^{186}\text{Os}$ ratio is thus large, and provides a sensitive handle on crust-mantle mixing. Despite the generally very low abundances (ppb range) of platinum group elements, the Re-Os system is by far the most interesting opportunity for micro-AMS in view of the demonstrated sensitivity for PGE detection by AMS, combined with the tediousness of chemical extraction of Re and Os required for conventional mass spectrometry. AMS offers an additional advantage for the Re/Os system: the negative elemental ions of Re are highly suppressed [18], reducing if not eliminating the isobaric interference effect. The large effect in the $^{187}\text{Os}/^{186}\text{Os}$ ratio, varying from ~ 1 for the mantle to ~ 14 in the crust (e.g., in Mn nodules), implies that even a few percent measurement would be useful. Ion microprobes have been used for direct measurement of the Os isotopes on PGE minerals (e.g., osmiridium) [35,36], where the Os contents are high. The generally low concentration of Os-Re (≥ 1 ppb) in rocks requires preconcentration techniques of which NiS fire-assay is the most commonly used [5,37]. In this process Re is collected with less efficiency than Os, which also helps to reduce the interference of ^{187}Re . Micro-AMS will facilitate direct measurements on minerals (other than platinum group minerals) which are known to concentrate PGE (e.g., molybdenite).

A number of prospective applications are presented in

Table 2
Geological tools from AUSTRALIS

Sulfides
Os isotopes as tracer: crustal/mantle reservoirs
PGE fractionation pattern as tracer
Pb isotopes as tracer
Re–Os dating of sulfide assemblages
Trace element partitioning between sulfide/silicates
Trace element zoning
Micas: Rb–Sr dating, Sr isotopes
Hydrous minerals: U–Pb dating

Table 2. The examples are not meant to represent an exhaustive list of potential applications, but rather to indicate areas where AUSTRALIS can be applied readily. Many other chronological systems need to be explored. Considerations discussed in Section 2 would preclude the use of some systems, e.g. $^{147}\text{Sm}/^{143}\text{Nd}$, where the required precision is in the 0.05‰ range. In contrast, the U/Pb and Re/Os systems with expected large variations in isotopic ratios are ideal candidates for first applications of AUSTRALIS.

6. Conclusion

Microbeam AMS presents a challenge in the technological development of AMS, but the anticipated rewards in geological applications are commensurate with the challenge. It will open up new windows of opportunity in basic as well as applied geology through in-situ microanalytical capability in ultra-trace element geochemistry and in isotope geology. It will enable high throughput data acquisition by simplifying sample preparation. The non-destructiveness (apart from micro-volume consumption of the sample) enables easier repeat analysis.

New applications are expected to arise from the ability of in-situ microanalysis for Pb isotopes in hydrous minerals, Sr isotopes in high Rb phases and the Os isotopes at low levels of abundance. Higher sensitivity for trace elements is expected to compete favourably with competing methods of conventional ion-microprobe and the laser ablation ICP-MS.

The microbeam and high precisions required in isotopic geology define constraints of applicability of the technique and puts a greater demand on the beam optics and stability of the ion source and beam transport elements.

Acknowledgements

The design and implementation of the project AUSTRALIS benefited greatly from our interaction with the

IsoTrace laboratory and the University of North Texas group, including M. Anthony from Texas Instruments, and G. Amsel's group at University Paris Sud.

References

- [1] L.K. Fifield, D. Fink, S.H. Sie and C. Tuniz, *AMS-6 Proc.*, Nucl. Instr. and Meth. 92 (1994).
- [2] J.C. Rucklidge, G.C. Wilson and L.R. Kilius, *Nucl. Instr. and Meth. B* 52 (1990) 507.
- [3] G. Chai, A.J. Naldrett, J.C. Rucklidge and L.R. Kilius, *Can. Miner.* 31 (1993) 19.
- [4] G.C. Wilson, L.R. Kilius and J.C. Rucklidge, *Geochim. Cosmochim. Acta* 55 (1991) 2241.
- [5] L.R. Kilius, N. Baba, M.A. Garwan, A.E. Litherland, M.J. Nadeau, J.C. Rucklidge, G.C. Wilson and X.L. Zhao, *Nucl. Instr. and Meth. B* 52 (1990) 357.
- [6] U. Fehn, R. Teng, D. Elmore and P.W. Kubik, *Nature* 323 (1986) 707.
- [7] R.T.D. Teng, U. Fehn, D. Elmore, T. Hemmick, P.W. Kubik and H.E. Gove, *Nucl. Instr. and Meth. B* 29 (1987) 281.
- [8] R.T.D. Teng, U. Fehn, D. Elmore, P.W. Kubik, T. Hemmick and H.E. Gove, *Lunar Planet. Sci.* 19 (1988) 1189.
- [9] S.J.B. Reed, *Miner. Mag.* 53 (1989) 3.
- [10] N. Shimizu, M.P. Semet and C.J. Allegre, *Geochim. Cosmochim. Acta* 42 (1978) 1321.
- [11] W. Compston, I.S. Williams and S.W.J. Clement, *Annu. Conf. Am. Soc. Mass Spectrom.* 30 (1982) 593.
- [12] N.S. Belshaw, R.K. O'Nions, D.J. Martel and K.W. Burton, *Chem. Geol.* 112 (1994) 57.
- [13] H. Matsuda, *Int. J. Mass Spectrom. Ion Phys.* 14 (1974) 219.
- [14] H. Matsuda, *Nucl. Instr. and Meth. A* 298 (1990) 199.
- [15] S.H. Sie and G.F. Suter, *Nucl. Instr. and Meth.* 92 (1994) 221.
- [16] S.H. Sie, T.R. Niklaus and G.F. Suter, in: *Proc. Heavy Ion Accelerator Technology Conf.*, Canberra, Nov. 1995. *Nucl. Instr. and Meth. A* 382 (1996) 299.
- [17] S.H. Sie, *Nucl. Instr. and Meth. B* 10/11 (1985) 664.
- [18] S.H. Sie, *Nucl. Instr. and Meth. B* 75 (1993) 403.
- [19] S.H. Sie, F. Leaney, R. Gillespie, G.F. Suter and C.G. Ryan, *Nucl. Instr. and Meth. B* 92 (1994) 35.
- [20] R. Middleton, *A Negative Ion Cookbook*, University of Pennsylvania, 1989, unpublished.
- [21] H. Liebl, *Nucl. Instr. and Meth.* 191 (1981) 183.
- [22] H. Liebl, *J. Phys. E* 8 (1975) 797.
- [23] H. Liebl, *J. Vac. Sci. Technol.* 12 (1975) 385.
- [24] M. Suter, G. Bonani, C. Steller and W. Woelfli, *Nucl. Instr. and Meth. B* 5 (1984) 251.
- [25] G. Amsel, E. D'Artemare and E. Girard, *Nucl. Instr. and Meth.* 205 (1983) 5.
- [26] K.J. Hansen and R. Lauer, in: *Focusing of Charged Particles*, vol. I, ed. A. Septier (Academic Press, New York, 1967) p. 251.
- [27] S.H. Sie, T.R. Niklaus and G.F. Suter, these Proceedings (AMS-7), *Nucl. Instr. and Meth. B* 123 (1997) 558.
- [28] D.A. Dahl and J.E. Delmore, SIMION for PC/PS2 vers. 4.0, EGG-CS-7233 Rev. 2, April 1988 and version 5.0 for extended DOS (1994).

- [29] A. Septier, in: *Focusing of Charged Particles*, vol. II, ed. A. Septier (Academic Press, New York, 1967) p. 123.
- [30] A. Havette and G. Slodzian, in: *Secondary Ion Mass Spectrometry – SIMS III*, eds. A. Benninghoven et al. (Springer, Berlin, 1982) p. 288.
- [31] G. Ray and S.R. Hart, *Int. J. Mass Spectrom.* 44 (1982) 231.
- [32] A.J. Walder, I.D. Abell, I. Platzner and P.A. Freeman, *Spectrochim. Acta* 48B (1993) 397.
- [33] G. Jenner, S.F. Foley, S.E. Jackson, T.H. Green, B.J. Fryer and H.P. Longerich, *Geochim. Cosmochim. Acta* 57 (1993) 5099.
- [34] R.A. Exley, *Earth. Planet. Sci. Lett.* 65 (1983) 303.
- [35] S.R. Hart and E.D. Kinloch, *Econ. Geol.* 84 (1989) 1651.
- [36] K. Hattori and L.J. Cabri, *Can. Miner.* 30 (1992) 289.
- [37] C.E. Martin, *Geochim. Cosmochim. Acta* 55 (1991) 1421.